DOCUMENTATION

ECCW

Exact Critical Coulomb Wedge

B.C.L. Mary

February 5, 2018

Summary

ECCW is a python library and a GUI of this library. The ECCW python library allows to compute the exact solution of critical Coulomb wedge, draw it, sketch it, with love. Are available compressive or extensive geological context, with or without fluid pore pressure.

Contents

1 Usage

```
main.py [-h] [-V] [-d] [-f FILE]
```

2 Understand ECCW

2.1 The critical coulomb wedge theory.

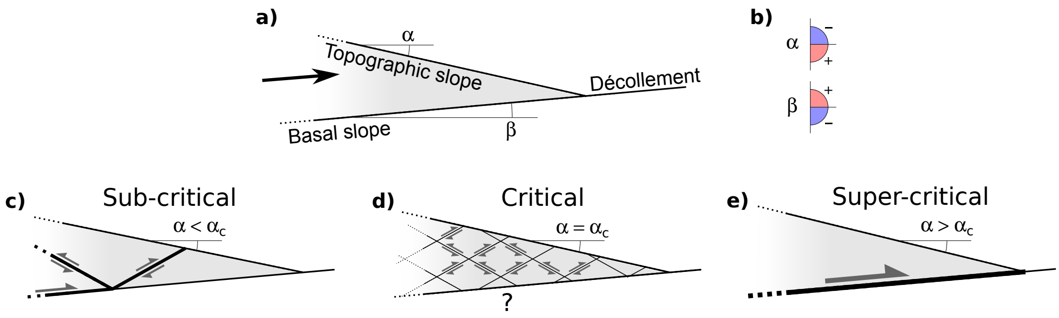

Figure 1

2.2 Criticality.

The critical enveloppe defines three domains of stability (see figure 4):

- Super-critical
- Sub-critical
- Critical

In the super-critial doamin, outside the enveloppes, no internal deformation occurs. The prism only slides on the basal décollement (figure 3). In the sub-critical domain, including the enveloppes, some internal deformations occurs. This deformation will appears along the pushing back-wall in the sub-critical domain (figure 2), while it can occurs *anywhere* inside the prism at the exact critical state.

2.3 Motor of faulting

Mathematically constituted of four parts due to the two arcsin included in the impicite solution (see section 3), the critical enveloppe is meaningfull by group of two. In all plots of this documentation, the enveloppe is drawed in two parts, highlited by the red and blue lines. The red line represent configurations where the faults are in reverse mode, while the configurations under the blue line are in normal mode (see Figure **??** and 1).

The "motor" of normal or reverse faulting is in all cases tectonic motion or gravitational collapse. According to the geological context, these "motors" are seted differently. For compressive context, reverse faulting (bottom red line) is driven by tectonic motion while normal faulting is due to gravitational collapse (Figure **??**). For extensive context this normal faulting (upper blue line) which is driven by tectonic motion and reverse faulting by gravitational collapse (Figure 1).

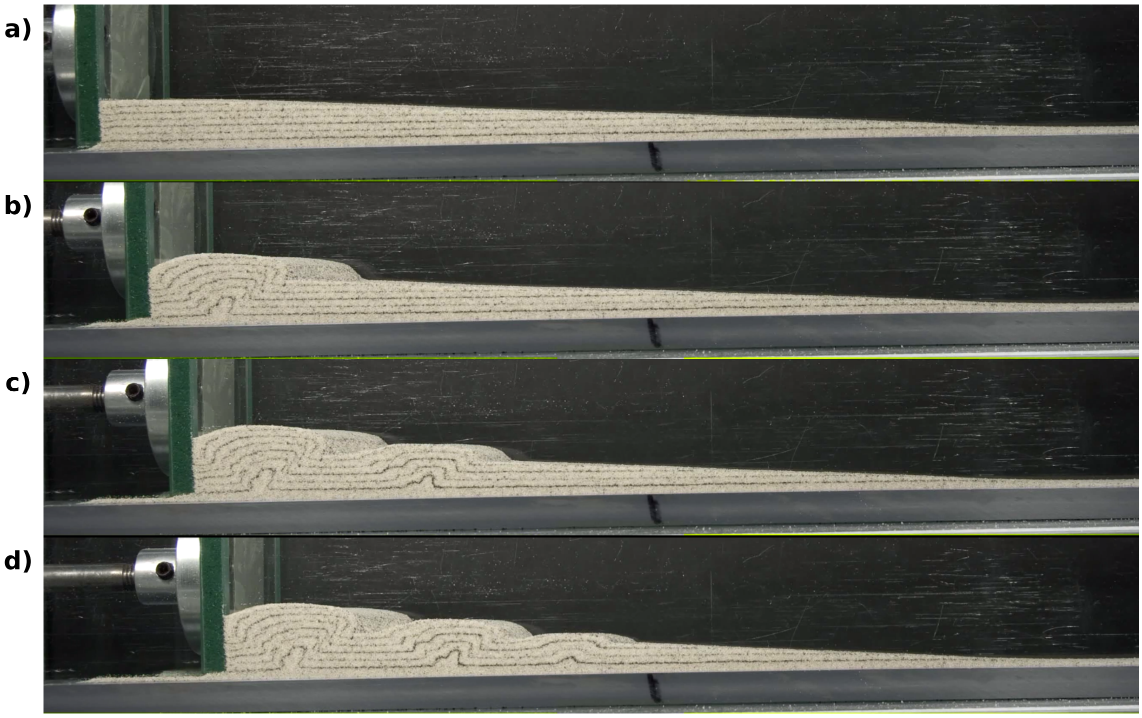

Figure 2: *Sandbox experiment showing deformation occuring in a prism initally at sub-critical state (**a**). Deformation is propagating from the back-wall to the front (**b** to **d**). After Souloumiac Thesis, 2009.*

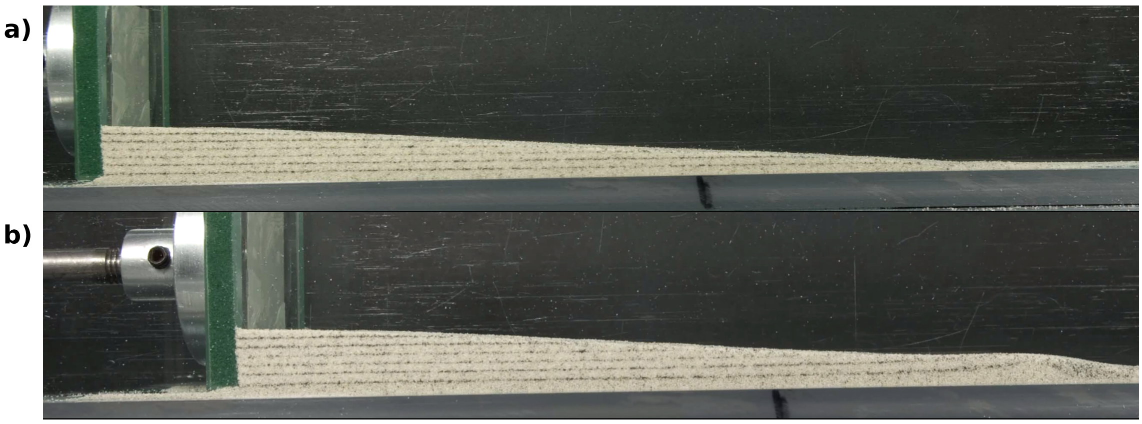

Figure 3: *Sandbox experiment showing no deformation occuring (**b**) in a prism initally at super-critical state (**a**). After Souloumiac Thesis, 2009.*

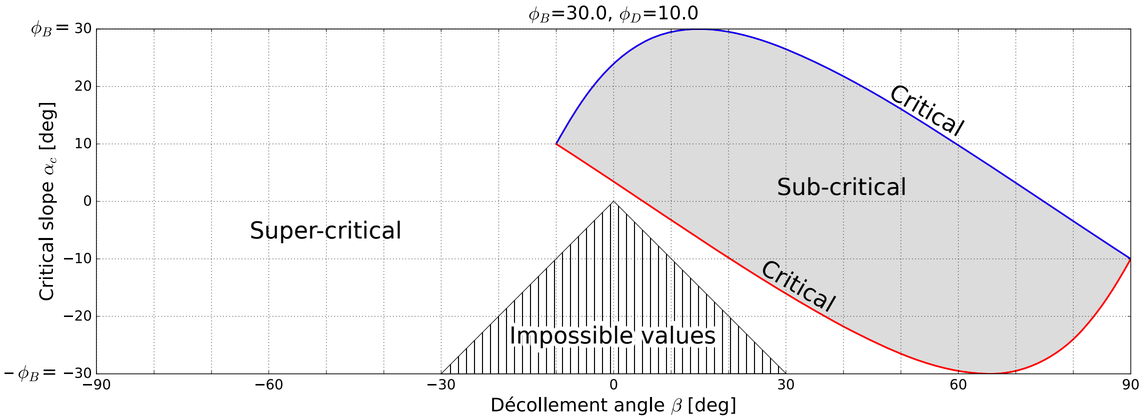

Figure 4: *The domains of stability defined by the critical enveloppes : deformation occurs in the prism if it lays in the sub-critical domain (gray surface), including the critical enveloppes (red and blue lines). No deformation occurs in the super-critical domain : the tectonic force is accomodated only by sliding on the basal décollement.*

3 Compute ECCW

3.1 Critical prism theory

From Dahlen [1984] and Yuan et al. [2015] we get a relation between the basal slope β and the topographic slope α of a frictional material pushed by an horizontal tectonic force.

3.2 The exact implicit solution

From [Yuan et al., 2015], we get :

$$\alpha_c + \beta = \Psi_D - \Psi_0 \tag{1}$$

with

$$\Psi_D = \frac{1}{2} \arcsin\left(\frac{(1-\lambda_D)\sin(\phi_D)}{(1-\lambda_B)\sin(\phi_B)} + \frac{\lambda_D - \lambda_B}{1-\lambda_B} \sin(\phi_D)\cos(2\Psi_0) \right) - \frac{1}{2}\phi_D \tag{2}$$

$$\Psi_0 = \frac{1}{2} \arcsin\left(\frac{\sin(\alpha_c')}{\sin(\phi_B)} \right) - \frac{1}{2}\alpha_c' \tag{3}$$

$$\alpha_c' = \arctan\left(\frac{1 - \frac{\rho_f}{\rho}}{1-\lambda_B} \tan(\alpha_c) \right) \tag{4}$$

3.3 Fault slopes at criticality

$$\theta_{A1} = \gamma_{A2} = \frac{\pi}{4} + \frac{\phi_B}{2} - \frac{1}{2}\arcsin\left(\frac{\sin(\alpha_c')}{\sin(\phi_B)} \right) - \frac{1}{2}\alpha_c' + \alpha_c \tag{5}$$

$$\gamma_{A1} = \theta_{A2} = \frac{\pi}{4} + \frac{\phi_B}{2} + \frac{1}{2}\arcsin\left(\frac{\sin(\alpha_c')}{\sin(\phi_B)} \right) + \frac{1}{2}\alpha_c' - \alpha_c \tag{6}$$

$$\theta_{B1} = \gamma_{B2} = \frac{\pi}{4} - \frac{\phi_B}{2} + \frac{1}{2}\arcsin\left(\frac{\sin(\alpha_c')}{\sin(\phi_B)} \right) - \frac{1}{2}\alpha_c' + \alpha_c \tag{7}$$

$$\gamma_{B1} = \theta_{B2} = \frac{\pi}{4} - \frac{\phi_B}{2} - \frac{1}{2}\arcsin\left(\frac{\sin(\alpha_c')}{\sin(\phi_B)} \right) + \frac{1}{2}\alpha_c' - \alpha_c \tag{8}$$

$$\max(\alpha_c) = -\min(\alpha_c) = \arctan\left(\frac{1-\lambda_B}{1-\frac{\rho_w}{\rho}}\tan(\phi_B)\right) \tag{9}$$

$$\tag{10}$$

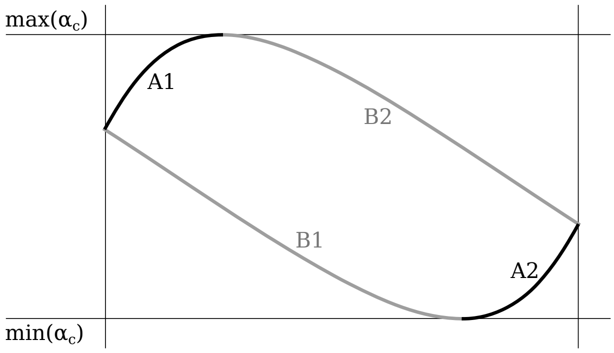

Figure 5: *The four mathematic domains of the critical enveloppes.*

3.4 Solve ECCW

An iterative method is necessary to solve ECCW. Here we had choose Newton's secant method. But some issues raise when one try to solve (1) directly due to the two arcsin included in (2) and (3). We choose here to rewrite equations (1), (2) and (3) into a set of three functions that should equals zero :

$$f_1 = \alpha_c + \beta - \Psi_D + \Psi_0 \tag{11}$$

$$f_2 = \sin(2\Psi_D + \phi_D) - \frac{(1-\lambda_D)\sin(\phi_D)}{(1-\lambda_B)\sin(\phi_B)} - \frac{\lambda_D - \lambda_B}{1-\lambda_B}\sin(\phi_D)\cos(2\Psi_0) \tag{12}$$

$$f_3 = \sin(2\Psi_0 + \alpha_c')\sin(\phi_B) - \sin(\alpha_c') \tag{13}$$

This set of equation can be used in an adapted form of the Newton's Method.

3.5 Newton's method

We use the Newton's secant method to iteratively converge towards the solution.
The iteration :

$$\Delta x = \frac{f(x_i)}{f'(x_i)} \tag{14}$$

with $\Delta_x = x_{i+1} - x_i$ and f' the derivative of f. Iterates until $\Delta x < \epsilon$, an arbitrary small threeshold. Initial value x_0 is given by user.
The derivative f' can be approximated using finite difference:

$$f'(x_i) = \frac{f(x_i) - f(x_{i-1})}{x_i - x_{i-1}} \tag{15}$$

or

$$f'(x_i) = \frac{f(x_i + h) - f(x_i)}{h} \tag{16}$$

with h a an arbitrary small value.

3.6 Adaptation of Newton's method to a set of functions

Let's define $\underline{F}$, a set of n functions :

$$\underline{F} = \begin{bmatrix} f_1(\underline{X}) \\ \vdots \\ f_n(\underline{X}) \end{bmatrix} \tag{17}$$

with $\underline{X} = x_1, \ldots, x_n$, n parameters. The derivative of each subfunction f_k is the sum of the partial derivative on $\underline{X}$. It is convenient for what follows to define $\underline{\underline{M}}$, a $n \times n$ matrix, constituted of partial derivative on $\underline{X}$ for columns, with lines dedicated to subfunctions :

$$\underline{\underline{M}} = \begin{bmatrix} \frac{\partial f_1}{\partial x_1} & \cdots & \frac{\partial f_1}{\partial x_n} \\ \vdots & \ddots & \vdots \\ \frac{\partial f_n}{\partial x_1} & \cdots & \frac{\partial f_n}{\partial x_n} \end{bmatrix} \tag{18}$$

Each elements of $\underline{\underline{M}}$ can be approximated using (15) or (16). For example, using (16) on a set of 3 equations function of $\underline{X} = (x, y, z)$, $\underline{\underline{M}}(\underline{X_i})$ is given by

$$\begin{bmatrix} \frac{f_1(x_i+h,y_i,z_i)-f_1(\underline{X_i})}{h} & \frac{f_1(x_i,y_i+h,z_i)-f_1(\underline{X_i})}{h} & \frac{f_1(x_i,y_i,z_i+h)-f_1(\underline{X_i})}{h} \\ \frac{f_2(x_i+h,y_i,z_i)-f_2(\underline{X_i})}{h} & \frac{f_2(x_i,y_i+h,z_i)-f_2(\underline{X_i})}{h} & \frac{f_2(x_i,y_i,z_i+h)-f_2(\underline{X_i})}{h} \\ \frac{f_3(x_i+h,y_i,z_i)-f_3(\underline{X_i})}{h} & \frac{f_3(x_i,y_i+h,z_i)-f_3(\underline{X_i})}{h} & \frac{f_3(x_i,y_i,z_i+h)-f_3(\underline{X_i})}{h} \end{bmatrix} \tag{19}$$

Using (17) and (18), we can now rewrite (14) :

$$\underline{\underline{M}} \cdot \Delta\underline{X} = -\underline{F} \tag{20}$$

$$\Delta\underline{X} = \underline{\underline{M}}^{-1} \cdot -\underline{F} \tag{21}$$

This last rewriting allows to solve 11, 12 and 13 by iteration, using $\underline{X} = (\beta, \Psi_0, \Psi_D)$.

References

Dahlen, F. A. (1984). Noncohesive critical coulomb wedges: An exact solution. *Journal of Geophysical Research*, 89(B12):10125–10133.

Yuan, X. P., Leroy, Y. M., and Maillot, B. (2015). Tectonic and gravity extensional collapses in overpressured cohesive and frictional wedges. *Journal of Geophysical Research: Solid Earth*, 120(3):1833–1854.